9K

Optimum Body Profiles with Minimum Drag in Two-Dimensional Oseen Flow

M. BESSHO, National Defense Academy, and

Y. HIMENO, University of Osaka Prefecture, Japan

ABSTRACT

The present paper deals with an inverse problem for obtaining optimum body profile with minimum drag in two-dimensional Oseen flow. The flow quantity is at first represented and determined by integral equations using Oseen kernel function and taking stresses on the body surface as variables. Then the variation of the drag due to a slight arbitrary deformation of the profile is calculated and expressed in terms of the flow quantities and the deformation vectors on the surface, also in an integral representation. A Newton-Raphson type iterative scheme is proposed to obtain an optimum distribution of the deformation vectors for mimimizing the drag. The treatment of multi-restriction condition is also described and several numerical results are shown.

NOMENCLATURE

A	Area of body profile
b	Half beam
B	Breadth
C	Body contour
Ci	Coefficients
D	External domain
E	Integral for reciprocity theorem
k	$= 1/(2\nu)$
K_0, K_1	Modified Bessel functions
l	Half length
L	Length
n	Normal coordinate to surface
N	Number of segments
p	Pressure
P,Q	Points (x,y) and (x',y')
Pi	Kernel function for pressure
r	Distance from P to Q
R	Drag of body
Rn	Reynolds number
s	Tangential coordinate along C
Ts,Tn	Stresses in s and n directions
u,v	Velocities in x and y directions
U	Uniform Velocity
Ui,Vi	Kernel functions for u and v
x,y	Coordinates of point P
x',y'	Coordinates of point Q
X,Y	Stresses in x and y directions
Xi,Yi	Kernel functions for X and Y
Zi	Kernel functions for vorticity
β	Beam-length ratio = B/L
δ	Prefix representing variation
ν	Kinematic viscosity
ρ	Fluid density
ζ	Vorticity
Superscript '	Different flow field
Superscript *	Reverse flow quantity
Subscript n,s	Derivatives or components in n and s directions
Subscript x,y	Derivatives w.r.t. x and y
Subscript i	Natural number (1 or 2)

1. INTRODUCTION

In the field of ship wave resistance, a variety of inverse methods for the improvement of ship hull form based on linear wave theory have been established and are widely used in ship design. In the ship viscous resistance field, on the other hand, very few work has been done yet, because of the difficulty of evaluating the viscous resistance itself. The present work is an attempt of fundamental approach to the inverse problem of drag minimization in Oseen flow field.

In early time Bessho (1) showed a method of minimizing crosswise potential flow energy in a ship section which was assumed to be related to ship viscous resistance and obtained optimum frame line configuration. Hess (2) proposed a scheme for obtaining optimum body shape in which he used Squire and Young's formula for evaluating viscous resistance. Nagamatsu (3) applied direct search method for the same optimization problem in which he used boundary layer calculation to determine the drag. Nowacki's recent work (4) also seems to be along this line although he applied his optimization technique to evaluate optimum ship dimensions with ordinary hull form. Such a method of nonlinear programming based on a ship boundary layer calculation will become a useful tool of practical ship design.

On the other hand, it would also be interesting to make fundamental analysis on drag minimization as a pure hydrodynamic problem. Recently Bessho (5) developed a scheme for optimizing boundary shape in boundary element

method in plane stress analysis and applied it to the problem of finding an opimized boundary shape with least stress concentration (6). The method was applied to a flow problem by Bessho and Kyozuka (7) to obtain a cavity shape. They also applied the method to a drag minimization problem based on an empirical boundary layer type formula to obtain optimum shapes in two--dimensional and axisymmetric flows (8,9). Bessho and Himeno (10,11) also applied the method to two-dimensional and axisymmetric Stokes flows to find optimum body shapes. The present work is an extention of the method to two-dimensional Oseen flow.

After Oseen's original work (12), Oseen flow has been studied from various points of view, for instance, Filon's infinite Reynolds number flow (13), Imai's solution (14) by multipole expansion method, Miyagi's integral equation method (15), and so on. Attempts of expanding Navier-Stokes equation by the use of Oseen's kernel function have recently been made by Bessho (16,17,18,19) and Kida (20). Therefore study on Oseen flow seems still to be useful for the understanding of viscous fluid flow.

The procedure of the present inverse method can briefly be stated as follows. The first step is an ordinary method for solving the flow quantities and the drag on a prescibed body shape by integral equation. The secod step is an inverse procedure in which the deviation of the drag due to a small deformation of the body shape is formulated and then inversely the deformation is solved so that the drag is minimized. The third step is an iterative scheme to deform the body profile and to return to the first step until it converges. Thus the present scheme can be regarded as a Newton-Raphson's method in which the drag is a nonlinear function of the body profile.

In the following chapter this scheme is applied to two-dimensional Oseen flow.

2. BASIC EQUATIONS AND RECIPROCITY THEOREM

2.1 Basic Equations

Let us consider a body contour C, the external domain D, and the interior domain $\bar{D}$ as shown in Fig.1. The uniform velocity U is supposed to be in the positive x direction. Let all stresses in the fluid be normalized by the fluid density ρ, then the basic 2-d Oseen equations can be written in terms of the perturbation velocityies u and v, and the pressure p,

$$\begin{aligned} Uu_x &= -p_x + \nu\nabla^2 u \\ Uv_x &= -p_y + \nu\nabla^2 v \end{aligned} \tag{1}$$

and

$$u_x + v_y = 0. \tag{2}$$

The adjoint equation which corresponds to the reverese flow can also be expressed in the following form by replacing U to -U.

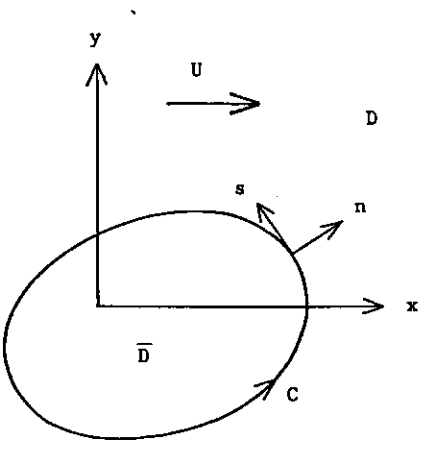

Fig.1 Coordinate system

$$\begin{aligned} -Uu^*_x &= -p^*_x + \nu\nabla^2 u^* \\ -Uv^*_x &= -p^*_y + \nu\nabla^2 v^* \end{aligned} \tag{3}$$

and

$$u^*_x + v^*_y = 0 \tag{4}$$

The boundary conditions are:

$$u = -U,\ v = 0,\ u^* = U,\ v^* = 0 \text{ on } C. \tag{5}$$

The stress components X and Y per unit length on arbitrary plane in D are defined as

$$\begin{pmatrix} X \\ Y \end{pmatrix} = \begin{pmatrix} -p+2\nu u_x, & (u_y+v_x) \\ (u_y+v_x), & -p+2\nu v_y \end{pmatrix} \begin{pmatrix} x_n \\ y_n \end{pmatrix} \tag{6}$$

where x_n and y_n represent directional cosines of the normal $\vec{n}$ of the plane. On C, eq.(6) can be transformed into the following form by using the boundary condition (5), the continuity (2), and the vorticity ζ ($= v_x - u_y$).

$$X = -px_n - \nu\zeta y_n,\quad Y = -py_n + \nu\zeta x_n \tag{7}$$

The tangential and normal components of the stress Ts and Tn on C become the form,

$$Ts = Xx_s + Yy_s = \nu\zeta,\quad Tn = Xx_n + Yy_n = -p. \tag{8}$$

Similar expressions also hold for the reverse flow quantity.

The relationship between the pressure and the vorticity on the contour C can be derived from equation (1) and the boundary conditions as follows.

$$p_n = -\nu\zeta_s,\quad p_s = \nu\zeta_n - \zeta x_n \tag{9}$$

The last term should disappear if we take Navier-Stokes equation instead of Oseen's one, so that the pressure and the vorticity are conjugate each other on C in real fluid.

Other flow properties in Oseen flow are well known through many text books, and are not stated here.

2.2 Reciprocity Theorem

Let us take two arbitrary velocity fields (u,v) and (u',v') in the domain D and introduce the following double integral E.

$$E(u,v;u',v') = \nu \iint_D 2(u_x u'_x + v_y v'_y) + (u_y + v_x)(u'_y + v'_x)\, dxdy \qquad (10)$$

The integral E would be related to the dissipation energy in the fluid if the two fields should coincide. It is obvious that reciprocity between the two fields holds in the expression E.

$$E(u,v;u',v') = E(u',v';u,v) \qquad (11)$$

If we assume (u,v) satisfies eq.(1) and (u',v') coincides with (u^*,v^*), i.e., the reverse Oseen flow in eq.(3), we can substitute these equations into eq.(10) and perform partial integration, by utilizing eq.(6). Then we can obtain a line integral form.

$$\int_C (u^*X + v^*Y)ds = \int_C (uX^* + vY^*)ds - U\int_C (uu^* + vv^*)ds \qquad (12)$$

If we apply the boundary condition (5), the last term vanishes and we obtain the form,

$$U\int_C X\, ds = -U\int_C X^* ds \qquad (13)$$

which means that the drags in the positive flow and in the reverse flow are the same, and that it is independent of the body shape.

2.3 Velocity Field

In eq.(12), the reverse flow velocities u^* and v^* can be replaced to the Oseen kernel functions like Ui(P,Q), Vi(P,Q), where the point P(x,y) lies on the boundary C and the singularity lies at the point Q(x',y') in the domain D. Thus we have

$$\begin{aligned} u(Q) &= -\int_C (X(P)U_1(P,Q) + Y(P)V_1(P,Q) \\ &\quad -u(P)X_1(P,Q) - v(P)Y_1(P,Q) \\ &\quad -(u(P)U_1(P,Q) + v(P)V_1(P,Q))x_n)ds(P), \\ v(Q) &= -\int_C (XU_2 + YV_2 - uX_2 - vY_2 - (uU_2 + vV_2)x_n)ds. \end{aligned} \qquad (14)$$

In eq.(14), the contour of the line integration has been extended to include a small circle around the singularity point Q, and the stress singularities Xi and Yi correspond to those of velocities Ui and Vi satisfying eq.(6). All of the singularities are listed in APPENDIX.

If the point Q lies inside of C, a similar expression to eq.(14) holds and then bringing the point Q to the external region D the left-hand side of the expression will be zero, which can be added to the original eq.(14). Then the result will be the following form in which the boundary condition is also taken into account.

$$\begin{aligned} u(Q) &= -\int_C (XU_1(P,Q) + YV_1(P,Q))ds(P) \\ v(Q) &= -\int_C (XU_2(P,Q) + YV_2(P,Q))ds(P) \end{aligned} \qquad (15)$$

Equation (15) holds in the entire domain $D+\bar{D}$, and means that the flow is at rest in the internal region. This is the fundamental expression for 2-d. Oseen flow with the stresses on the surface as unknown variables.

If the point Q lies on C, we have a set of integral equations for solving the stresses X(P) and Y(P) on C.

$$\begin{aligned} \int_C X(P)U_1(P,Q) + Y(P)V_1(P,Q)\, ds(P) &= 1 \\ \int_C X(P)U_2(P,Q) + Y(P)V_2(P,Q)\, ds(P) &= 0 \end{aligned} \qquad (16)$$

Eq.(16) can be solved by any numerical scheme. Then we can determine the flow quantities, the velocities by eq.(15), and the vorticity and the pressure by the following equations.

$$\zeta(Q) = -\int_C (XZ_1(P,Q) + YZ_2(P,Q))ds(P) \qquad (17)$$

$$p(Q) = -\int_C (XP_1(P,Q) + YP_2(P,Q))ds(P) \qquad (18)$$

It should be noted here that in eqs.(15) to (18) the pressure constant p_0 remains undetermined, which can be fixed by prescribing the pressure inside of C to be zero, for instance.

From the procedure mentioned above, we can evaluate all the flow quantities once the body profile is prescribed. This is the first step of the present inverse analysis.

3. BODY DEFORMATION AND DRAG MINIMIZATION

3.1 Drag Variation Due to Body Deformation

Let us assume that the body profile is deformed by an amount of δn in the normal direction to the contour C as shown in Fig. 2. The new domain is denoted as D', and correspondingly the velocities become u' and v', which can be analytically continued to the original contour C if the deformation is very small. We can define velocity variations δu and δv on C and approximate them to the first order as in the following form.

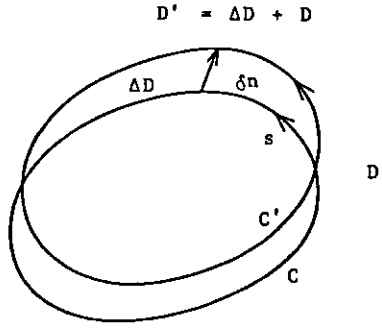

Fig.2 Body deformation

$$\delta u = u'(\text{on } C) - u(\text{on } C) = -u_n(\text{on } C)\delta n = \zeta_y \delta n, \text{ on } C$$
$$\delta v = -v_n \delta n = -\zeta_x \delta n \tag{19}$$

Similar expression also holds for the reverse flow velocities u* and v*.

The drag R can be defined by using the reciprocity integral (10) as the following form.

$$UR = U\int_C X ds = -E_D(u,v;u^*,v^*) - U\iint_D (u^* u_x + v^* v_x)dxdy \tag{20}$$

The drag R' in the new domain D' can also be defined by putting the prime ' to all the quantities in eq.(20). Thus the deviation of the drag δR due to δn can be defined as

$$\delta R = R' - R \tag{21}$$

and utilizing the definition of R and R' we obtain the following form.

$$U\delta R = I_1 + I_2 \tag{22}$$

$$I_1 = E_D(u,v;u^*,v^*) + U\iint_D (u^* u_x + v^* v_x)dxdy \tag{23}$$

$$I_2 = E_D(u,v;u^*,v^*) - E_D(u',v';u^{*\prime},v^{*\prime}) - U\iint_D (u^{*\prime}u_x' + v^{*\prime}v_x' - u^* u_x - v^* v_x)dxdy \tag{24}$$

The first integral (23) represents the effect of deviation of the domain, whereas the second integral (24) corresponds to the effect of the velocity change due to the body deformation.

After reduction and linearization of the above equations we can first obtain the form,

$$I_1 = \int_C (\nu\zeta\zeta^* + U^2 u_x)\delta n \, ds \tag{25}$$

in which the vorticity definition and the continuity equation on C are used for the derivation. And for the second integral we can make partial integration of eq.(24) and obtain

$$I_2 = \int_C (u^{*\prime}X' + v^{*\prime}Y' - u^* X - v^* Y)\, ds = \int_C (\delta u^* X + \delta v^* Y + u^* \delta X + v^* \delta Y)\, ds. \tag{26}$$

For the deviations of the stresses X and Y in eq.(26), we can use the following equation as a variation of eq.(12).

$$\int_C (u^*\delta X + v^*\delta Y)ds = \int_C (\delta u X^* + \delta v Y^*)ds - U\int_C (u^*\delta u + v^*\delta v)x_n \, ds \tag{27}$$

Substituting eq.(27) into eq.(26), and using eq.(19) we finally obtain the form for the second integral.

$$I_2 = -\int_C (2\nu\zeta\zeta^* - U^2 u_x)\delta n \, ds \tag{28}$$

The expression for the drag variation δR is consequently derived in the following form,

$$U\,\delta R = -\int_C (\nu\zeta\zeta^* - 2U^2 u_x)\delta n \, ds \tag{29}$$

where the first term in the righthand side corresponds to the same expression in Stokes flow (Bessho and Himeno, 10), and the last term to an inertia effect. Similar equation can be obtained for the drag variation δR* in the reverse flow,

$$U\,\delta R^* = +\int_C (\nu\zeta\zeta^* - 2U^2 u_x^*)\delta n \, ds \tag{30}$$

and from eq.(13)

$$\delta R + \delta R^* = 0. \tag{31}$$

Combining these three equations we finally obtain the following form.

$$\int_C (\zeta - \zeta^*)x_n y_n \delta n \, ds = 0 \tag{32}$$

$$U\delta R = -\int_C (\nu\zeta\zeta^* + U^2(\zeta+\zeta^*)x_n y_n)\delta n \, ds \tag{33}$$

3.2 Drag Minimization

An optimum profile in the present problem should have minimum drag, so that the variation of the drag should be zero.

$$U\delta R = -\int_C (\nu\zeta\zeta^* - 2U^2 u_x)\delta n \, ds = 0 \tag{34}$$

As the least requirement for the restriction condition, we assume here the area A of the body profile to be specified as a constant, which means that the variation δA becomes zero.

$$\delta A = \int_C \delta n \, ds = 0 \tag{35}$$

Therefore from eqs.(34) and (35) we obtain

$$\nu\zeta\zeta^* - 2U^2 u_x = \text{const.} = C_0 \tag{36}$$

or,

$$\nu\zeta\zeta^* + (\zeta+\zeta^*)x_n y_n = C_0 \tag{37}$$

It is noted that as the viscosity increases only the first term remains, which corresponds to the case in Stokes flow. In the high Reynolds number range, however, eq.(36) becomes

$$u_x = \text{const. on } C \tag{38}$$

which will lead to meaningless solution because of the boundary condition, i.e., lead to a numerical divergence in the solution procedure.

The edge angle of the optimum body can also be analyzed in the same manner as in Stokes flow, and the requirement condition at the edge is found to be a finite value for the vorticity which results that the half edge angle is proved to be 51.3 degree, same to Stokes flow, though the proof is omitted here.

3.3 Iterative Solution Procedure

Since eq.(36) or (37) is nonlinear for the unknown vorticities, we cannot solve the equation system directly. An iterative scheme is required to obtain the optimum profile. Let us take a deviation of eq.(37), then we obtain the

form,

$$\delta\zeta(\nu\zeta^*+x_n y_n)+\delta\zeta^*(\nu\zeta+x_n y_n) = C_0 - \nu\zeta\zeta^*-(\zeta+\zeta^*)x_n y_n, \text{ on C} \quad (39)$$

where the variations of the vorticity $\delta\zeta$ and $\delta\zeta^*$ are related to the variations of the stress using eq.(17).

$$\delta\zeta = -\int_C(\delta XZ_1(P,Q)+\delta YZ_2(P,Q))ds, \text{ on C} \quad (40)$$

Similar relation holds for the reverse flow. We can also take the variation of eq.(15) for the velocity, and substitute it into eq.(19).

$$\delta u = -\int_C(\delta XU_1+\delta YV_1)ds = \zeta y_n \delta n$$
$$\delta v = -\int_C(\delta XU_2+\delta YV_2)ds = -\zeta x_n \delta n \quad (41)$$

Therefore, once we obtained the flow quantities on a prescibed initial body profile, we can obtain the variations of the stresses δX and δY, the linearized optimum body deformation n, and the unknown constant C , by solving eq.(35) and eqs.(39) to (41) at the same time. We would also have to combine the similar expressions for the reverse flow if the body shape should be asymmetric. All the equations are in integral form so that they can be converted into a set of simultaneous equations. And the kernel functions are almost the same to those in solving the flow quantities.

After the deformation vector is obtained on the body contour, we can deform the profile and obain a new shape as the next step. This procedure should be iterated until it converges within a prescribed error allowance.

In case that the body profile is symmetric about the origin, a great deal of the reduction of the number of the unknowns can be made. We thus have

$$\zeta(x,y)= -\zeta(-x,y),\ \zeta^*(x,y)= -\zeta^*(-x,y)$$
$$\delta n(x,y)= \delta n(-x,y) \quad (42)$$

and eq.(32) is satisfied automatically. So the unknowns are distributed only in the upper quadrants of C and it is not necessary to calculate the reverse flow quantity.

3.4 Multi-Restriction Condition

It is not difficult to introduce other type of restriction condition. The length of the body can be specified in the following form.

$$\delta n(y=0) = 0 \quad (43)$$

The beam can also be specified as

$$\delta n(x=0) = 0 \quad (44)$$

in case of symmetric body.

Any other condition like the above can be added to the original equations for determining the deformation vector, although eq.(37) should be changed to include additional terms in order to compansate the increased number of equation. Thus we may assume

$$\nu\zeta\zeta^*+(\zeta+\zeta^*)x_n y_n = C_0 + C_1x^2+ C_2x^4+.. \quad (45)$$

Considering eq.(34), the additional terms in eq.(45) correspond to the conditions for specifying higher order moments of the profile such as the following forms, in the after body.

$$\int_C x^2\delta n\, ds = 0, \quad \int_C x^4\delta n\, ds = 0 \ ,,,. \quad (46)$$

We thus have additional unknown coefficients for the additional restriction conditions.

4. NUMERICAL PROCEDURE

4.1 Panel Method

For the first step of the inverse analysis in the 2-d. Oseen flow, only right-left and fore-aft symmetric body profile is treated here. The contour C in the upper plane is divided into N segments (N is about 30), on which the variables are assumed to be constant. When the area is to be specified, the value is taken to be the same to that of a circle of unit radius, i.e., π. For solving eq.(16) to determine the flow field, the number of the unknowns is 2N for the stresses X and Y in the upper plane. And for determining the deformation vector, 2N unknowns for δX and δY in the upper plane, N/2 for δn in the first quadrant, and a few unknowns for the additional conditions are needed. All the integral equations are transformed into simultaneous linear equations and are solved by Gauss-Jordan method with double precision digit.

The initial profile for the iteration is prescribed as an ellipse with an appropriate beam-length ratio. The number of the iteration is from 5 to 20 according to the initial shape and to the error allowance for convergence, which is about 0.003 for max. of δn.

4.2 Singularity Treatment

As will be shown in APPENDIX, all the Oseen kernels like Ui, Vi, Zi, Pi includes the modified Bessel functions of the zeroth and first orders, $K_0(kr)$ and $K_1(kr)$, where $k=1/2\nu$, and r denotes the distance between the points P and Q. For small kr we have

$$K_0(kr) = -\log(kr) + O(1) \quad (47)$$

$$K_1(kr) = 1/(kr) + O(kr). \quad (48)$$

These singularities can be treated only in self-induced segment (P=Q), in which the singular part is analytially integrated and the rest is treated by Gaussian numerical integration.

For high Reynolds number, an asymptotic expansion for the Bessel functions can be utilized for larger value of kr.

$$K_0(kr) = K_1(kr) = (\pi/2kr)^{1/2}\exp(-kr) \quad (49)$$

Singular behavior like step function appears in

the wake region of a segment, which can be treated separately both for the upper and lower parts in the wake. This effect becomes severe when the segment lies parallel to x-axis and kr becomes large.

5. CALCULATION RESULTS AND DISCUSSIONS

5.1 Flow Around Elliptic Cylinder

Before proceeding to optimum profiles, it is useful to calculate the Oseen flow around elliptic cylinders in order to understand the flow property and to confirm numerical accuracy.

Fig.3 shows the Reynolds number effect on the pressure and vorticity distributions on the circular cylinder. As Reynolds number increases the stagnation pressure and the vorticity peak decreases and approaches to Filon's limiting flow. This situation also holds for an elliptic cylinder of beam-length ratio B/L=0.3 as shown in Fig.4. The drag coefficient for elliptic cylinders of various B/L ratio is calculated and shown in Fig.5. When the length L is specified there is no optimum B/L ratio with minimum drag so that flat plate has smallest drag for any Reynolds number. However when the area is specified there is an optimum B/L ratio in very small Reynolds number range, though the figure is not shown here. For moderate Reynolds number, therefore, the flat plate has smallest drag among the elliptic cylinders of same length or same area in Oseen flow.

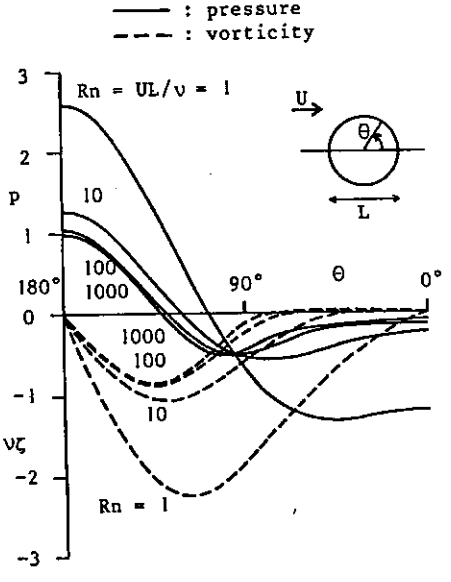

Fig.3 Pressure and vorticity distribution on circular cylinder

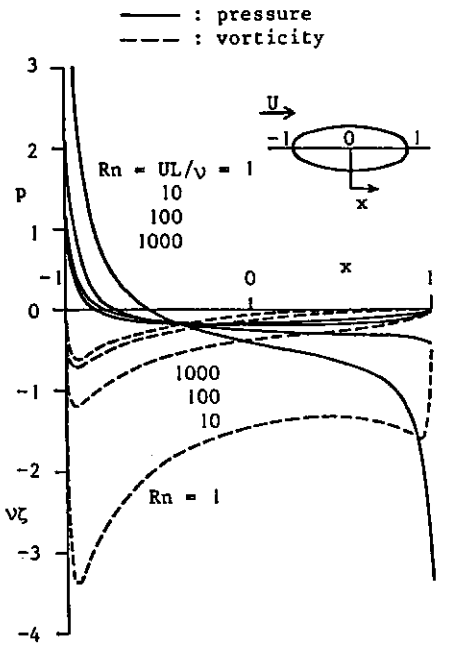

Fig.4 Pressure and vorticity distribution on elliptic cylinder (B/L = 0.3)

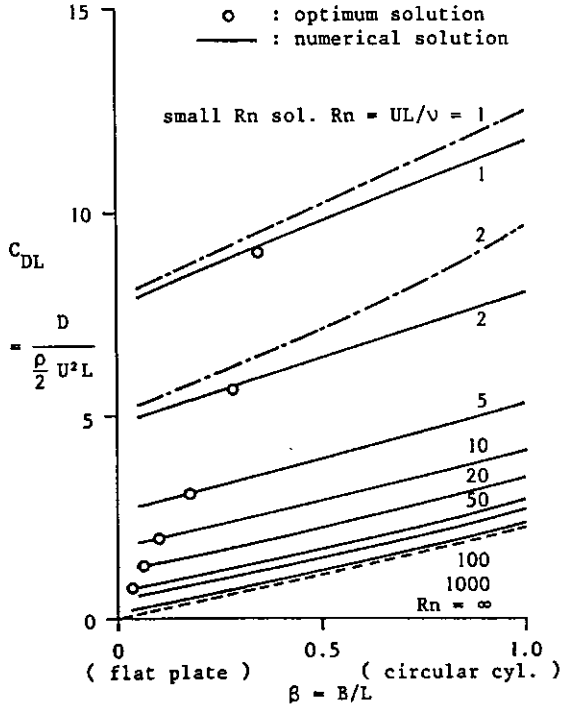

Fig.5 Drag coefficient of elliptic cylinders

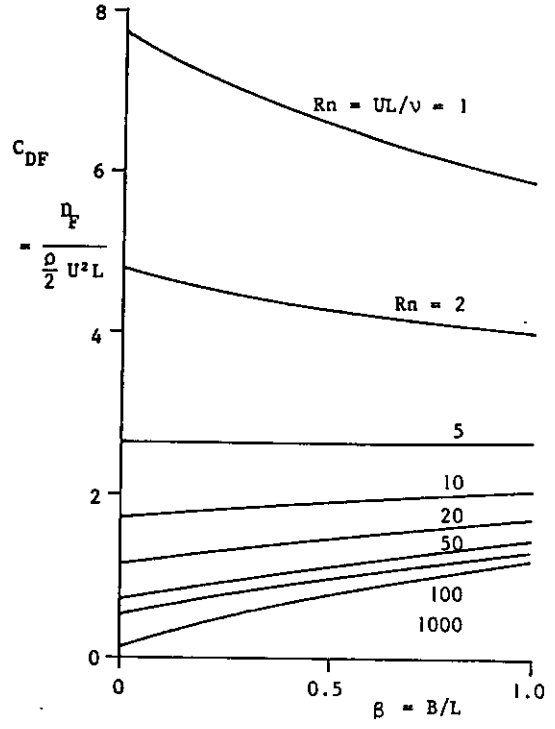

Fig.6 Friction drag coefficient

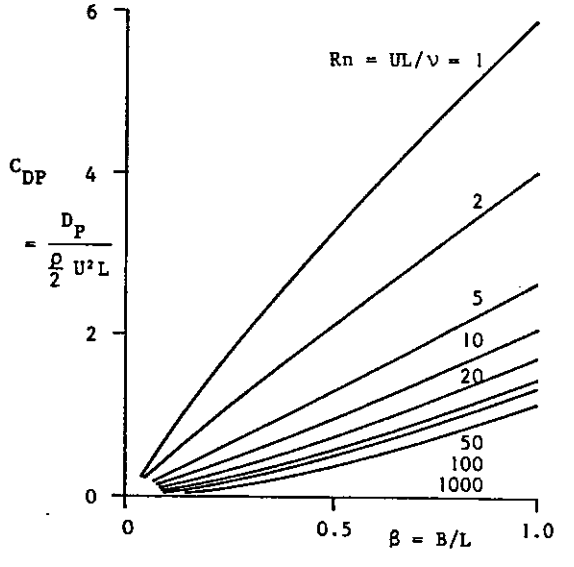

Fig.7 Pressure drag coefficient

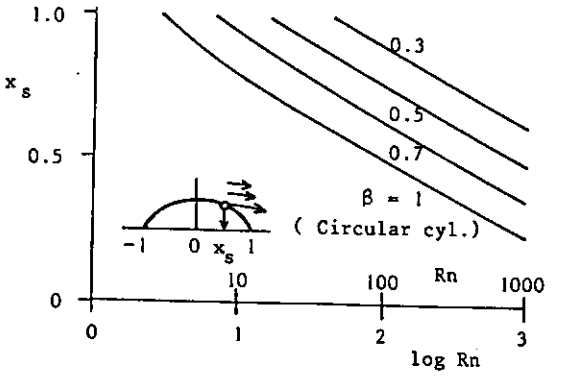

Fig.8 Location of separation point

Optimum B/L points for the optimum profile which will be stated later, are also plotted in Fig.5. Optimum profiles have a little smaller drag than the elliptic cylinder of same B/L ratio and also approach to flat plate as Reynolds number increases.

Figs. 5 and 6 illustrate the friction and pressure drag coefficients of the elliptic cylinders. The friction drag does not show rapid change against B/L and at high Reynolds number it seems to be proportional to B/L. The pressure drag, on the contrary, seems roughly proportional to the beam at moderate Reynolds number. For the relationship between the friction and pressure drags, the following formula

$$D_P = (B/L)\, D_F \qquad (50)$$

is numerically confirmed for elliptic cylinder at arbitrary Reynolds number in 2-d. Oseen flow, although the proof has not been done here.

The location of the separation point on the elliptic cylinders are shown in Fig.8. As Reynolds number increases the separation point moves upstream and approaches to maximum beam position, i.e., to the limiting flow pattern.

5.2 Optimum Profiles

The calculation is made here only for the symmetric profiles about origin, for simplicity and for the first step of the present problem.

Fig.9 shows the calculated results of elementary optimum profiles which have one ristriction condition, for instance, the area being specified to be π, same to that of the circular cylinder of unit radius. Only the first quadrant is shown in the figure. All the profiles have sharp edge at both ends where the half edge angle should be 51.3 degree according to the theoretical analysis. As Reynolds number increases the shape becomes elongated and approaches to flat plate.

The case when the length is specified to be 2 is shown in Fig.10. The Reynolds number dependency is similar to the former case of area specified. The profile should also be

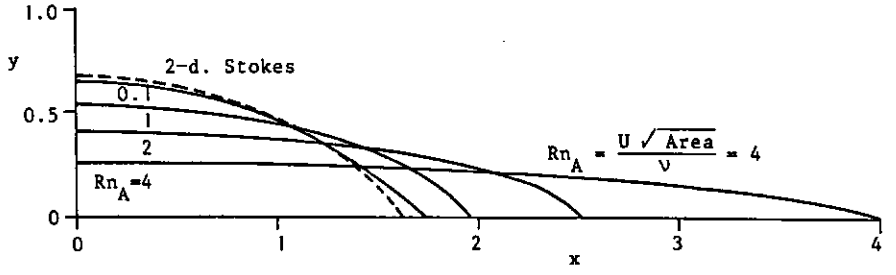

Fig.9 Optimum shape in 2-d. Oseen flow (Area = π)

similar to the former case when the corresponding Reynolds number is the same, since the same equation (37) is adopted for thr requirement of the vorticity. The drag has already been shown in Fig.5, where the drag reduction is quite small compared to that of elliptic cylinder of same B/L ratio.

Fig.11 shows the pressure and vorticity distribution on the profile, which has similar tendency to that of elliptic cylinder in Fig.4, although the vorticity has finite value at both ends of the profile. Fig.12 shows the half beam value which tends to that of Stokes flow (abt 0.4) for small Renolds number and approaches to zero, i.e., flat plate. The profile curve is normalized by the half beam and by the half length as shown in Fig.13. The normalized profiles in Oseen flow is somewhat elongated probably by the influence of the inertia term, compared to that in Stoke flow.

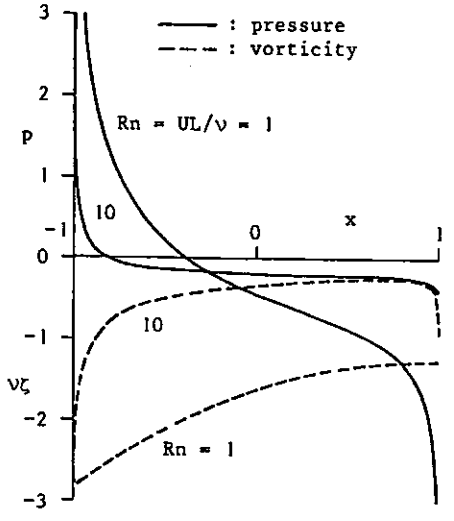

Fig.11 Pressure and vorticity distributions on optimum profiles

5.3 Optimum Profiles with Multi-Restriction

When the number of the ristriction condition is increased the freedom of deformability decreases as experienced in the Stokes flow problem. Here only the results with the length and the beam specified are shown as examples of the multi-restriction case. The length is fixed to be 2 in all cases and the beam is specified to be the value of the elementary optimum profile for a prescribed Reynolds number.

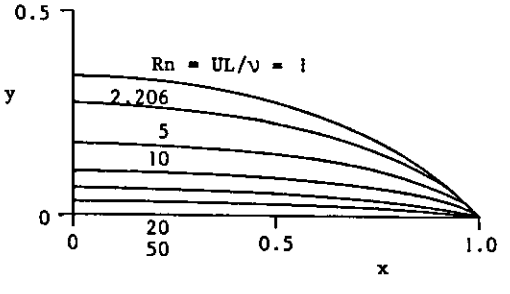

Fig.10 Optimum shape in 2-d. Oseen flow (fore-aft symmetric and length-specified)

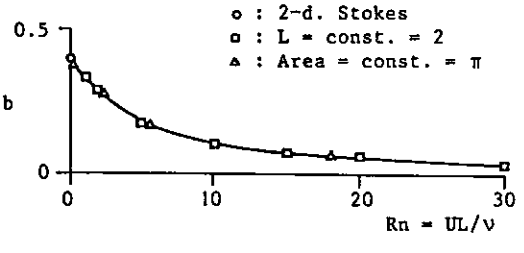

Fig.12 Half beam of optimum shape (L = 2.0)

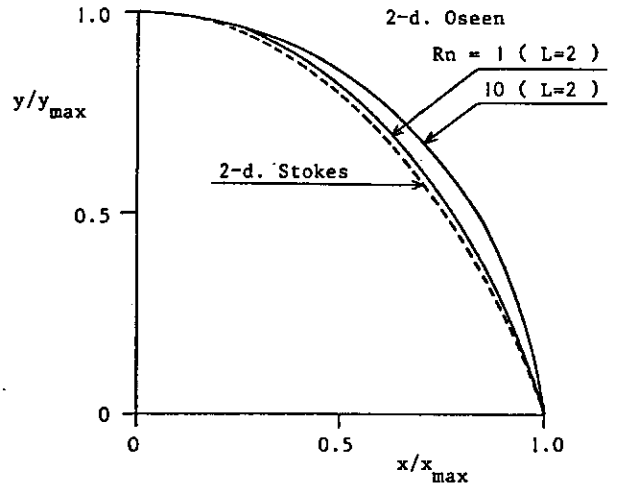

Fig.13 Normalized optimum shape

Figs.14 and 15 show the cases when the half beams are fixed to be 0.343 and 0.287 which correspond to the optimum values for the elementary optimum shape at Reynolds numbers 1 and 2 respectively. When Reynolds number increases with length and beam fixed, profiles with blunt nose are obtained and at higher Reynolds number the iteration does not converge. It can be considered that the blunt nose is a numerical solution with a cirtain accuracy and it may not be an exact solution, since the half nose angle must be 51.3 degree if the vorticity remains finite there. Therefore the appearance of the blunt nose seems to be due to the non-uniqueness of the solution at high Reynolds number. In any case, the increase of drag near the separated end for the blunt-nose profile seems to compensate with the drag decrease in the smoothened side area. A similar situation was also experienced in Bessho and Kyozuka's analysis on the optimum profiles based on the boundary layer concept (8).

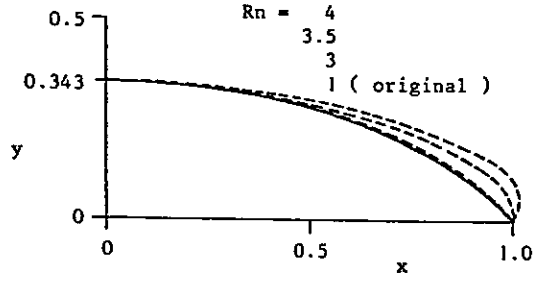

Fig.14 Optimum profiles (l=1, b=0.343)

The cases when narrower beams are specified are shown in Figs.16 to 18. The beams correspond to the elementary solutions at higher Reynolds number. When the beam becomes smaller, the blunt nose no longer appears and convergence is not achieved at high Reynolds number. Instead, round curves appear in the side region at lower Reynolds number. This is a quite similar result to that of Stokes flow (10) with multi-restriction.

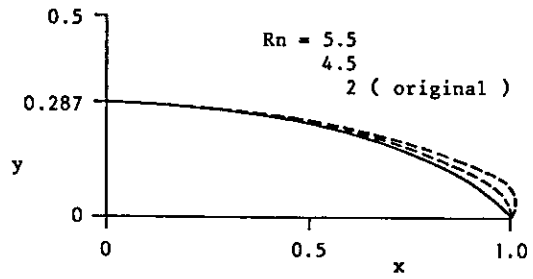

Fig.15 Optimum profiles (l=1, b=0.287)

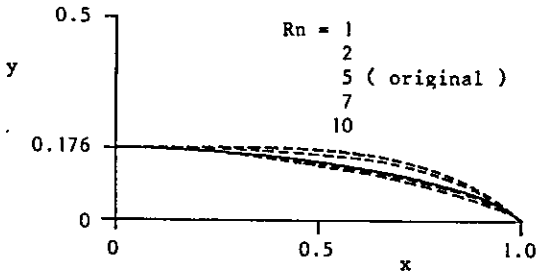

Fig.16 Optimum profiles (l=1, b=0.176)

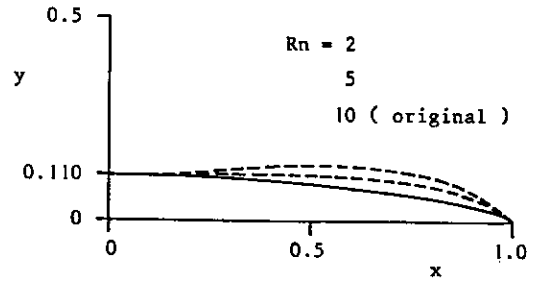

Fig.17 Optimum profiles (l=1, b=0.110)

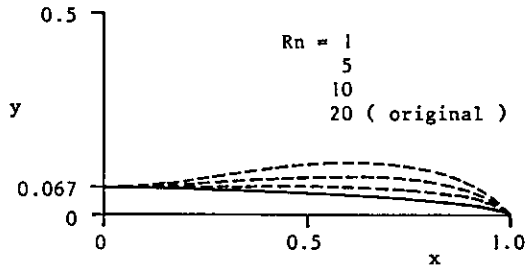

Fig.18 Optimum profiles (l=1, b=0.067)

6. CONCLUSIONS

Bessho's inverse scheme for obtaining optimum boundary shape by boundary element method is applied to two-dimensional Oseen flow. The optimum profiles with minimum drag are obtained in case of symmetric body. The following conclusions can be made.

i) In case when the area is specified the optimum profile becomes rather elongated than that in Stokes flow, and approaches to flat plate at high Reynolds number.

ii) The optimum profile has sharp edge at both ends where the half angle is 51.3 deg.

iii) For the case of the length specified similar results are obtained.

iv) When multi-restriction is specified, blunt-nose shapes are numerically obtained for the case of relatively large beam specified. For smaller beams, on the contrary, round shape in the side region appears which are similar to that in Stokes Flow.

v) All the iterative calculation do not converge at High Reynold number.

Further studies should be necessary on the asymmetric optimum profiles, axisymmetric case, application of the present scheme to Navier-Stokes flow, and so on.

REFERENCES

1. Bessho, M., "Study into Frame Line Configuration," Jour. Soc. Naval Archi. Japan, Vol.122, 1967 (in Japanese)

2. Hess, J. L., "On the problem of shaping an axi-symmetric body to obtain low drag at large Reynolds numbers," Jour. Ship Res., Vol.20, No.1, 1976

3. Nagamatsu, T. et al., "Study on the Minimization of Ship viscous Resistance," Jour. Soc. Naval Archi. Japan, Vol.154, 1983

4. Nowacki, H., "Optimization Methods Applied to Viscous Drag Reduction," Proc., Osaka Int. Coll., Osaka, 1985

5. Bessho, M. and Kawabe, H., "Singularity Method in Boundary Value Problem in the Theory of Elasticity," Part 1, Kansai Soc. Naval Archi., Japan, No.177, 1980 (in Japanese)

6. Bessho, M., "On the Stress Intensity Factor in the Erasto-Dynamics," Kansai Soc. Naval Archi., Japan, No.189, 1983 (in Japanese)

7. Bessho, M., Kyozuka, Y., et al., "On a Computation of Riabouchinski's Axi-Symmetric Cavity Flow," Trans. West-Japan Soc. Naval Archi., No.67, 1984 (in Japanese)

8. Bessho, M., Kyozuka, Y., et al., "Study into the Shape of Minimum Viscous Resistance," 1st Report, Trans. West-Japan Soc. Naval Archi. No.68, 1984 (in Japanese)

9. Bessho, M., Kyozuka, Y., et al., "Study into the Shape of Minimum Viscous Resistance," 2nd Report, Trans. West-Japan Soc. Naval Archi. No.70, 1985 (in Japanese)

10. Bessho, M. and Himeno, Y., "On Optimum Profiles in Two-Dimensional Stokes Flow," Jour. Kansai Soc. Naval Archi., Japan, No.193, 1984 (in Japanese)

11. Bessho, M. and Himeno, Y., "Study on Drag Minimization in Stokes Flow," Proc., 2nd Int. Symp. Ship Viscous Resist., Gothenberg, 1985

12. Oseen, C. W., "Hydrodynamik", Akad. Ver., Leipzig, 1927

13. Filon, L. N. G., "The Forces on a Cylinder in a Stream od Viscous Fluid," Proc. Roy. Soc., Ser.A, Vol.113, 1926

14. Imai, I., "A new method of solving Oseen's equation and its application to the flow past an inclined elliptic cylinder," Proc. Roy. Soc., Ser.A, Vol.224, 1954

15. Miyagi, T., "Oseen flow past a Circular Cylinder at High Reynolds Number," Jour. Phys. Soc. Japan, Vol.37, No.6 1974

16. Bessho, M., "Study of Viscous Flow by Oseen's Scheme," 1st Report, Jour. Soc. Naval Archi. Japan, No.156, 1984 (in Japanese)

17. Bessho, M., "Study of Viscous Flow by Oseen's Scheme," 2nd Report, Jour. Soc. Naval Archi. Japan, No.157, 1985 (in Japanese)

18. Bessho, M., "Study of Viscous Flow by Oseen's Scheme," 3rd Report, Jour. Soc. Naval Archi. Japan, No.158, 1985 (in Japanese)

19. Bessho, M., "On the Viscous Flow around A Thin Cylinders," Proc. Osaka Int. Colloquium on Ship Viscous Flow, Osaka, 1985

20. Kida, T., "A New Perturbation Approach to the Laminar Fluid Flow Behind a Two-Dimensional Solid Body," Soc. Ind. Appl. Mech., Jour. Appl. Math., Vol.44, No.5, 1984

APPENDIX: OSEEN'S KERNEL FUNCTIONS

The kernel functions in the 2-d. Oseen flow is well known and the following expressions are adopted here, in which the coefficients are determined so as to make the integral of the stress kernel X_1 around the point Q be unity.

$$2\pi U_1(P,Q) = (\ln r + F)_x + 2kF \qquad (51)$$

$$2\pi U_2 = 2\pi V_1 = (\ln r + F)_y \qquad (52)$$

$$2\pi V_2 = -(\ln r + F)_x \qquad (53)$$

In the above,

$$r^2 = (x-x')^2 + (y-y')^2 \qquad (54)$$

$$F(P,Q) = K_0(kr)\exp(k(x'-x)) \tag{55}$$

$$k = 1/(2\nu) \tag{56}$$

where K_0 is modified Bessel function of zeroth order. The kernel functions for pressure can be derived by taking harmonic part of the velocity kernel.

$$2\pi P_1(P,Q) = -(\ln r)_x \tag{57}$$

$$2\pi P_2(P,Q) = -(\ln r)_y \tag{58}$$

And the vorticity kernel is defined as

$$Z_i(P,Q) = V_i(P,Q)_{x'} - U_i(P,Q)_{y'} \tag{59}$$

so that we obtain

$$2\nu\pi Z_1(P,Q) = F_y \tag{60}$$

$$2\nu\pi Z_2(P,Q) = -F_x. \tag{61}$$

The kernels for the stresses can be derived from eq.(6) in the preceeing chapter.

DISCUSSION

William B. Morgan,
David W.Taylor Naval Ship R&D Center

From your work on optimum body profiles, can you give any guidance into the optimization of body profiles in turbulent flows? And, do you see any possibility of extension of your techniques to these flows?

Reply -

Thank you for the discussion. The key point of the present method is whether variational expressions both for the flow and the drag are possible or not. Therefore a direct extension of the present method to the real turbulent flows seems to be difficult. As cited in the references in the paper, however, an extension is possible if we use an approximate formula from turbulent boundary layer theory to obtain the drag, like Squire and Young's formula. Another possibility of this method is an extension to Navier-Stokes flow, on which Bessho has recently made some progress. The result would appear in the near future.

Dr. Jacek S. Pawlowski,
Institute for Marine Dynamics, NRCC,

I share the authors' interest in inverse hydrodynamic problems and therefore I have found their paper most interesting. I would like to point out that the inverse problems can be understood in a broader sense as problems of optimum form description rather than finding the optimum geometrical form for a particular regime of motions [a]. In practice the form of a body can rarely be optimized with respect to one hydrodynamic force, besides it seems that the optimum form description approach leads to a richer mathematical structure.

[a] Jacek S. Pawlowski, Form Parameters for Ship Design, Based upon Hydrodynamic Theory, International Symposium on Ship Hydrodynamics and Energy Saving, El Pardo, September 6-9, 1983.

Reply -

As you pointed out, it would be important to take many parameters into account for the purpose of finding optimum ship form in actual ship design. However, the aim of the present work is not such a practical application but is to offer a basic feature of the problem of finding the body form of minimized drag in viscous fluid flow. We believe that this kind of basic study would provide a physical base of understanding real flow to ship-form designers.